ELSEVIER

Thermochimica Acta 403 (2003) 153–160

thermochimica acta

www.elsevier.com/locate/tca

Low-temperature thermal properties of $Pb_2P_2Se_6$ and $Pb_{1.424}Sn_{0.576}P_2Se_6$

Keiichi Moriya [a,*], Tekehiro Yamada [a], Shipra Baluja [b], Takasuke Matsuo [c], Ivan Pritz [d], Yulian M. Vysochanskii [d]

[a] *Department of Chemistry, Faculty of Engineering, Gifu University, Yanagido, Gifu 501-1193, Japan*
[b] *Department of Chemistry, Saurashtra University, Rajkot 360005, Gujarat, India*
[c] *Department of Chemistry, Graduated School of Science, Osaka University, Toyonaka, Osaka 560-0043, Japan*
[d] *Institute for Solid State Physics and Chemistry, Uzhgorod University Pidgrina str., 46, Uzhgorod 294000, Ukraine*

Received 8 March 2002; accepted 21 October 2002

Abstract

The heat capacities of $Pb_2P_2Se_6$ and $Pb_{1.424}Sn_{0.576}P_2Se_6$ were measured at temperatures between 10 and 320 K for the former and between 10 and 330 K for the latter. The heat capacities values were analyzed by harmonic approximation using the Debye and Einstein functions. They were calculated using 3 Debye and 7, 7, 7, 6 Einstein sets. The calculated heat capacities were in good agreement with the observed ones.

Keywords: Heat capacity; Debye temperature; Einstein temperature; Lead diphosphoselenate; Lead–tin diphosphoselenate mixed crystal

1. Introduction

The Einstein [1] and Debye [2] theories of harmonic solids have been successfully used in a qualitative discussion of the thermodynamic properties of solids. It is now established that the thermal properties of a solid can be accurately calculated with in the harmonic approximation once the distribution function of the normal mode frequencies is known [3].

From an experimental point of view, we are often interested in the anomalous heat capacities such as those due to phase transitions and want to separate them from the vibrational heat capacity. For such purposes, the simple Debye and Einstein functions are easy to use and apparently give reasonable results. In a previous paper, we showed that the systematized use of the Debye and Einstein functions for a relatively complex coordination compound gives good consistency between the experimental and calculated heat capacities [4].

$Pb_2P_2Se_6$ and $Sn_2P_2Se_6$ crystals have an isomorphous monoclinic form with a space group of $P2_1/c$ at room temperature and form solid solutions at any proportion [5]. $Sn_2P_2Se_6$ transforms at 220 K to an intermediate incommensurate phase [6] and then transforms to a commensurate ferroelectric phase of the space group Pc with $z = 2$ at 193 K [7,8]. Isomorphism suggests the possibility of a phase transition in $Pb_2P_2Se_6$ but none has been reported. If $Pb_2P_2Se_6$ has no phase transition below room temperature, its heat capacity may be well reproduced by using the Debye and Einstein functions. The relatively large anharmonic contribution to the heat capacity at constant

* Corresponding author.
E-mail address: moriya@apchem.gifu-u.ac.jp (K. Moriya).

0040-6031/02/$ – see front matter
PII: S0040-6031(02)00510-5

volume occurs at high temperatures [9,10]. However, in this case, we are able to neglect this anharmonicity because the melting point is ca. 1050 K for the $Pb_2P_2Se_6$ crystals and the anharmonic contribution is at most a few percent of the $C_p - C_v$ correction at the high-temperature end of 300 K.

In the present paper, we report the heat capacities of $Pb_2P_2Se_6$ and $Pb_{1.424}Sn_{0.576}P_2Se_6$ and describe the analysis using the harmonic oscillator heat capacity functions.

2. Experiments

The heat capcities were measured with an adiabatic calorimeter between 10 and 330 K. The temperature of the cell was measured with a rhodium–iron resistance thermometer calibrated in terms of ITS-90. Precision of the heat capacity measurement was ±0.1% in the temperature range above 50 K, and the estimated accuracy was ±1% at 20 K and 0.3% above 50 K. Details of the calorimetric apparatus were previously described [11,12]. The sample crystals of $Pb_2P_2Se_6$ and $Pb_{1.424}Sn_{0.576}P_2Se_6$ weighed 8.5593 g (9.0087 mmol) and 3.4107 g (3.7932 mmol), respectively. The $Pb_2P_2Se_6$ and $Pb_{1.424}Sn_{0.576}P_2Se_6$ crystals were prepared by the Bridgemann method by slowly pulling up the single crystal from the melt containing the appropriate amounts of the elements. The compositions of the samples were determined using inductively coupled plazma–atomic emission spectroscopy (ICP–AES) for Sn and P and using atomic absorption spectroscopy (AAS) for Pb after the samples were dissolved in HCl/H_2O_2 solution. The ICP–AES and AAS were measured using Perkin-Elmer ICP 5500 and Nippon Jarrell Ash A 825 spectrometers. The compositions obtained for Pb, Sn and P, and the optimized mole fraction, x, in the $Pb_{2x}Sn_{2(1-x)}P_2Se_6$ single crystals are shown in Table 1.

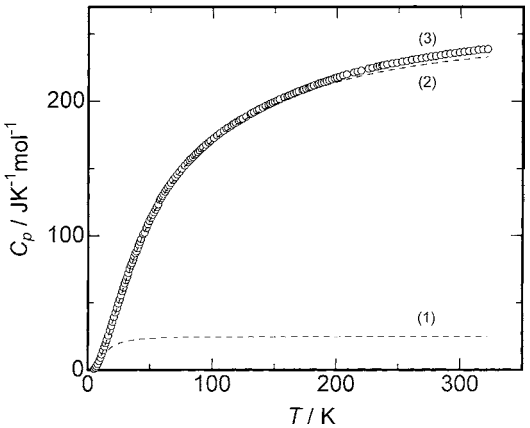

Fig. 1. Molar heat capacities of $Pb_2P_2Se_6$. The curves represent the calculated heat capacities. (1) Optimized Debye term. (2) Optimized Debye and Einstein terms. The calculated vibrational heat capacities at constant pressure. (3) Experimental molar heat capacities, open circles. The calculated heat capacities at constant pressure agree with the experimental values well within the size of the circles representing the latter.

3. Discussion

The heat capacities smoothly varied with temperature as shown in Figs. 1 and 2 and Tables 2 and 3 for $Pb_2P_2Se_6$ and $Pb_{1.424}Sn_{0.576}P_2Se_6$, respectively and no heat capacity anomaly corresponding to a phase transition was observed. The heat capacities are less dependent on temperature at room temperature and above, following the general course of the temperature dependence of the vibrational heat capacity characterized by low-frequency modes. The absence of the heat capacity anomaly in the $Pb_2P_2Se_6$ and $Pb_{1.424}Sn_{0.576}P_2Se_6$ crystals suggests that their heat capacities may be reproduced by a collection of harmonic oscillator contributions.

Table 1
The elemental analysis and Pb^{2+}ion mole fraction, x, in $Pb_{2x}Sn_{2(1-x)}P_2Se_6$ crystals

x	Pb		Sn		P	
	Calculated	Observed	Calculated	Observed	Calculated	Observed
0.712	33.3	32.8	8.1	7.6	6.8	6.9
1.000	43.6	46.1	–	–	6.5	6.3

Table 2
Experimental molar heat capacities of $Pb_2P_2Se_6$

T (K)	C_p ($J K^{-1} mol^{-1}$)	T (K)	C_p ($J K^{-1} mol^{-1}$)	T (K)	C_p ($J K^{-1} mol^{-1}$)	T (K)	C_p ($J K^{-1} mol^{-1}$)
5.147	0.9128	26.65	55.53	89.38	163.7	190.28	214.4
5.282	1.017	27.68	58.53	90.80	165.0	191.51	215.1
5.520	1.195	28.67	61.31	92.20	166.1	193.63	215.7
5.717	1.363	29.62	64.52	93.05	166.8	195.81	216.2
5.866	1.523	30.52	67.02	94.30	167.8	198.03	217.1
6.088	1.744	31.55	69.40	95.29	168.6	199.92	217.7
6.233	1.920	32.50	72.26	96.53	169.5	202.11	218.3
6.415	2.128	33.44	75.37	98.01	170.7	204.97	219.2
6.635	2.420	34.38	77.89	99.49	171.7	207.84	220.0
6.717	2.434	35.30	79.66	100.99	172.8	213.64	221.4
7.027	2.973	36.19	82.01	101.96	173.7	216.56	222.2
7.030	2.958	37.13	84.53	103.42	174.6	219.49	222.8
7.362	3.429	38.10	86.96	104.18	175.4	225.41	224.3
7.448	3.614	39.05	88.45	105.56	176.3	228.39	225.0
7.690	3.935	39.98	90.73	107.10	177.2	272.02	232.6
7.901	4.378	40.90	93.39	108.62	178.3	275.90	233.2
8.007	4.501	41.80	95.54	109.55	178.8	279.76	233.7
8.327	5.130	42.69	97.62	110.83	179.9	283.61	234.3
8.356	5.193	44.45	101.3	112.22	180.5	287.45	235.0
8.739	5.923	45.54	102.4	113.42	181.3	291.28	235.6
8.787	6.046	46.85	105.9	114.88	182.1	295.10	235.9
9.104	6.680	48.13	108.7	116.65	183.3	298.91	236.4
9.324	7.152	49.38	111.2	118.29	184.1	302.71	236.8
9.571	7.697	50.61	113.4	119.72	185.1	306.49	237.3
9.919	8.490	51.82	115.7	120.78	185.5	310.27	237.6
10.18	9.107	53.01	117.6	121.95	186.4	314.04	238.3
10.52	9.916	54.18	119.5	123.81	187.2	317.80	238.5
10.78	10.55	55.34	121.6	124.95	187.8	321.55	238.8
11.15	11.47	56.49	123.5	126.64	188.8	157.31	203.0
11.34	11.88	57.77	126.8	128.66	189.9	159.87	203.8
11.80	13.08	58.49	128.0	130.07	190.6	161.15	204.5
11.86	13.21	59.62	129.8	130.92	191.0	163.09	205.3
12.36	14.49	60.75	131.3	132.86	191.9	165.04	206.0
12.56	15.00	61.88	133.0	135.44	193.4	167.00	206.8
12.88	15.89	63.01	134.7	137.07	194.1	168.97	207.6
13.44	17.37	64.14	136.2	138.85	194.8	171.95	208.5
13.96	18.81	65.27	137.8	139.99	195.4	172.96	208.9
14.31	19.79	66.66	139.6	142.28	196.6	174.97	209.6
14.99	21.65	68.32	141.8	144.58	197.5	176.99	210.2
15.16	22.25	69.97	143.8	146.09	198.2	178.03	210.7
16.25	25.29	71.60	145.7	146.89	198.6	232.36	225.8
16.44	25.69	73.23	147.6	147.93	199.0	234.39	226.3
17.52	28.90	75.19	149.9	149.78	199.7	236.40	226.7
17.70	29.36	77.48	152.4	151.65	200.6	237.42	226.8
18.70	32.41	79.74	154.7	153.52	201.5	240.46	227.6
18.84	32.84	81.28	156.3	179.03	211.0	244.44	228.1
19.88	35.78	82.58	157.6	181.08	211.8	248.43	228.8
21.05	39.40	83.91	158.8	183.14	212.6	252.40	229.5
22.18	42.78	85.25	160.0	184.14	212.6	256.35	230.0
23.31	46.10	86.40	161.2	185.21	213.1	260.29	230.8
24.47	49.52	87.99	162.5	187.30	213.8	264.22	231.5
25.58	52.57	88.59	163.1	189.40	214.2	268.12	232.0

Table 3
Experimental molar heat capacities of $Pb_{1.424}Sn_{0.576}P_2Se_6$

T (K)	C_p ($J K^{-1} mol^{-1}$)	T (K)	C_p ($J K^{-1} mol^{-1}$)	T (K)	C_p ($J K^{-1} mol^{-1}$)	T (K)	C_p ($J K^{-1} mol^{-1}$)
6.342	2.471	21.38	39.63	96.19	168.7	214.62	221.1
6.543	2.663	21.87	41.06	98.81	170.8	217.48	222.1
6.765	2.956	22.35	42.54	101.51	172.8	309.71	237.7
7.035	3.374	23.31	45.34	104.19	174.7	312.54	237.9
7.159	3.552	24.26	48.04	106.85	176.7	315.98	238.3
7.618	4.302	25.21	50.81	109.50	178.4	220.34	222.8
8.128	5.151	26.26	53.68	112.13	180.1	223.20	223.4
8.226	5.333	27.41	57.26	114.75	181.6	226.07	224.2
8.753	6.339	28.53	60.48	117.36	183.1	228.94	224.9
8.789	6.387	29.63	63.79	119.96	184.6	231.81	226.3
9.321	7.464	30.70	66.78	122.55	186.0	234.69	226.2
9.533	7.910	31.76	69.53	125.14	187.3	237.57	226.8
9.830	8.544	32.94	72.67	127.72	188.5	240.46	227.3
10.32	9.603	34.39	76.62	130.30	190.0	243.35	228.2
10.87	10.83	35.95	80.89	132.88	191.4	246.25	228.3
11.01	11.31	37.46	84.78	135.46	192.6	249.16	228.8
11.46	12.24	38.93	88.31	138.04	194.0	252.07	229.4
11.76	13.02	40.36	91.72	140.62	195.3	254.99	229.9
12.03	13.64	41.75	95.05	143.20	196.4	257.91	230.5
12.54	14.96	43.12	98.02	145.78	197.4	260.84	231.1
12.57	15.00	44.47	101.1	148.37	198.6	263.77	231.5
13.10	16.37	46.15	104.8	151.07	199.8	266.44	231.7
13.46	17.29	48.13	108.9	153.88	201.1	266.71	232.3
13.61	17.77	50.29	113.1	156.69	202.2	269.76	232.1
14.11	19.02	52.61	117.3	159.50	203.3	273.67	232.5
14.38	19.73	54.83	121.3	162.32	204.4	277.58	233.0
14.60	20.28	56.99	124.9	165.14	205.6	281.50	233.8
15.25	22.08	59.08	128.5	167.97	206.6	285.43	234.2
15.27	22.14	59.55	129.1	170.80	207.6	289.36	235.0
16.07	24.40	62.20	133.0	173.64	208.8	293.31	235.6
16.08	24.41	64.45	136.2	176.49	209.7	297.26	235.9
16.84	26.52	66.81	139.3	179.34	210.6	301.22	236.8
16.88	26.67	69.17	142.3	182.20	211.6	305.19	237.1
17.58	28.63	71.54	145.2	185.04	212.5	307.46	237.5
17.65	28.73	74.00	148.1	187.92	213.3	309.17	237.2
18.40	30.81	76.54	150.9	190.88	214.3	319.40	238.7
18.47	31.21	79.03	153.6	193.88	215.2	322.82	239.0
19.12	33.04	81.48	156.0	196.89	215.9	326.24	239.4
19.42	33.87	83.90	158.1	199.89	217.0	329.64	239.9
19.83	34.98	86.29	160.5	202.89	218.3	333.04	240.3
20.41	36.85	88.65	162.8	205.87	219.1	336.43	240.7
20.52	37.09	91.11	164.8	208.85	220.0	339.82	241.3
21.20	39.32	93.66	166.8	211.77	220.5		

3.1. Model heat capacity function

The model heat capacity function consisted of three parts: $C(1)$ and $C(2)$, the heat capacity due to acoustic and optical lattice vibrations whose characteristic temperatures are determined by comparison with the heat capacity data, and $C(3)$ small correction terms for the difference between C_p and C_v. For the calculation of $C(1)$, the following Debye heat capacity function was used;

$$C(1) = R \sum_{i=1}^{N_D(1)} g_{Di}(1) C_D \left(\frac{\Theta_{Di}(1)}{T} \right) \quad (1)$$

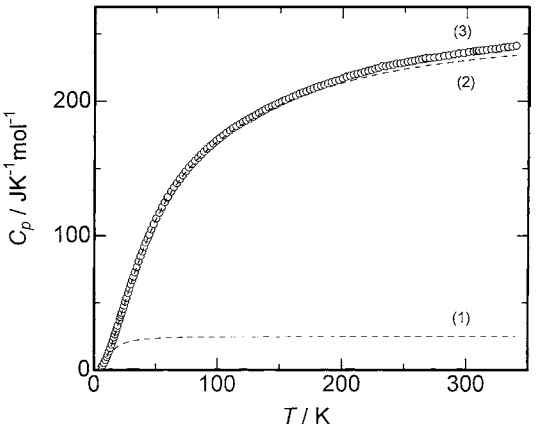

Fig. 2. Molar heat capacities of $Pb_{1.424}Sn_{0.576}P_2Se_6$. The curves represent the calculated heat capacities. (1) Optimized Debye term. (2) Optimized Debye and Einstein terms. The calculated vibrational heat capacities at constant pressure. (3) Experimental molar heat capacities, open circles. The calculated heat capacities at constant pressure agree with the experimental values well within the size of the circles representing the latter.

where R is the gas constant and $g_{Di}(1)$ the weights of the contributions from the respective terms. Θ_{Di} is the Debye temperature in order to be optimized by the least square method to reproduce the experimental heat capacities. We chose $N_D(1) = 1$, and $g_{D1}(1) = 3$.

The Debye heat capacity function was computed using a series expansion [13],

$$C_D = \frac{4\pi^4}{5x^3} - \sum(3(nx) + 12 + 36/nx + 72(nx)^2 + 72(nx)^3)\frac{e^{-nx}}{n} \quad (2)$$

where $x = \Theta_D/T$. The infinite series was truncated in the actual calculation at an approximate number of terms.

$C(2)$, which is the heat capacity due to optical lattice vibrations, was calculated using the following equation:

$$C(2) = R\sum_{i=1}^{N_E(2)} g_{Ei}(2)C_E\left(\frac{\Theta_{Ei}(2)}{T}\right) \quad (3)$$

where C_E is the Einstein heat capacity function and g_{Ei} (2) the weights of the contribution from the Einstein function. The sum of the weights, g_{Ei} (2) ($i = 1$ to $N_E(2)$) and $g_{D1}(1)$ ($i = 1$ to $N_D(1)$) equates the number of the vibrational degrees of freedom. Since there are $N = 10$ atoms in the chemical formula unit for $Pb_2P_2Se_6$ and $Pb_{1.424}Sn_{0.576}P_2Se_6$, they sum to 30.

Thus,

$$3N = \sum_{i=1}^{N_D(1)} g_{D1}(1) + \sum_{i=1}^{N_E(2)} g_{Ei}(2) \quad (4)$$

We chose $N_D(1) = 1$, $g_{D1}(1) = 3$, $N_E(2) = 4$, $g_{E1}(2) = 7$, $g_{E2}(2) = 7$, $g_{E3}(2) = 7$ and $g_{E4}(2) = 6$. The first term contains 3 d.f. and the second term 27.

The Einstein heat capacity function normalized to 1 at $T = \infty$ is written as follows:

$$C_E(x) = \frac{x^2e^{-x}}{(1-e^{-x})^2} \quad (5)$$

where $x = \Theta_E/T$ and a total of 27 d.f. were included in $C(2)$.

The $C(3)$ part is the $C_p - C_v$ correction term and it was written as $VT\beta^2/\kappa$, where β and κ are the volume thermal expansion and volume compressibility coefficients of the samples. The $Pb_2P_2Se_6$ is monoclinic and β and κ must be replaced by the thermal expansion tensor, a_λ ($\lambda = 1 \sim 6$) and the compliance tensor, $s_{\lambda\mu}(\lambda, \mu = 1 \sim 6)$. When we use the isothermal stiffness coefficient, $c_{T\lambda\mu}$ instead of the compliance tensor, the $C_p - C_v$ term is written as follows:

$$C_p - C_v = TV\sum_{\lambda=1}^{6}\sum_{\mu=1}^{6} c_{T\lambda\mu}\alpha_\lambda\alpha_\mu \quad (6)$$

The temperature dependence of the isothermal stiffness coefficient is very small and the temperature dependence of the thermal expansion tensor is very close to that of the heat capacity at constant pressure at low temperatures [14]. When we assume that the temperature dependence of the isothermal stiffness coefficients is neglected and the thermal expansion coefficients are proportional to the heat capacity at constant pressure, the $C_p - C_v$ term is written by the next equation

$$C_p - C_v = AC_p^2T \quad (7)$$

where A is one of the least squares parameters. This equation is based on thermodynamics using quasi harmonic approximation [15].

Table 4
The best-fit values of the Debye and Einstein temperatures and A coefficient determined from 10 to 320 K data-set

$\theta_D(3)$ (K)	$\theta_{E1}(7)$ (K)	$\theta_{E2}(7)$ (K)	$\theta_{E3}(7)$ (K)	$\theta_{E4}(6)$ (K)	A (mol J^{-1})
55.0 ± 0.3	81.4 ± 0.4	152.3 ± 1.5	222.7 ± 2.1	612 ± 10	(3.38 ± 1.0) $\times 10^{-7}$

Table 5
The best-fit values of the Debye and Einstein temperatures and A coefficient determined from 10 to 330 K data-set

$\theta_D(3)$ (K)	$\theta_{E1}(7)$ (K)	$\theta_{E2}(7)$ (K)	$\theta_{E3}(7)$ (K)	$\theta_{E4}(6)$ (K)	A (mol J^{-1})
53.0 ± 0.3	84.6 ± 0.4	148.2 ± 1.4	226.8 ± 2.1	612 ± 10	(3.55 ± 1.0) $\times 10^{-7}$

3.2. Optimization and its result

The parameters $\Theta_{Di}(1)$ ($i = 1$), $\Theta_{Ei}(2)$ ($i = 1$–3) and A were optimized by minimizing the following function:

$$F(\Theta_{Di}(1),\ \Theta_{Ei}(2),\ A) = \sum_{i=1}^{N_{DA}} \{C_{exp}(T_i) - C_{calc}(T_i)\}^2 \quad (8)$$

$$C_{calc}(T_i) = C(1) + C(2) + A(C_{exp}(T_i))^2 T_i \quad (9)$$

where N_{DA} is the number of the experimental points taken into the fitting. The search for the best fit parameters were performed using a personal computer in which the program was written in BASIC. The algorithm was based on the iterated solution of the linearized normal equation.

The best fit functions are shown in Figs. 1 and 2 for $Pb_2P_2Se_6$ and $Pb_{1.424}Sn_{0.576}P_2Se_6$ along with the experimental data, respectively (see Appendix for calculated data). $C(1)$ (the Debye term) and $C(1)+C(2)$ (the Einstein term) are shown as dotted lines in the figures. Tables 4 and 5 give the best fit set of parameters for the data-points between 10 and 320 K for $Pb_2P_2Se_6$ and

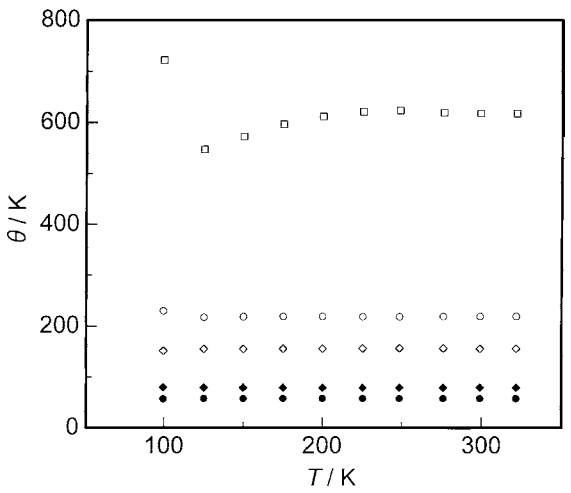

Fig. 3. The best-fit parameter values as functions of the data-set used for fitting $Pb_2P_2Se_6$. The horizontal axis represents the upper end temperature of the interval of the data-set. The lower end temperature was 13 K for all the points. Probable errors are roughly equal to the size of the circles.

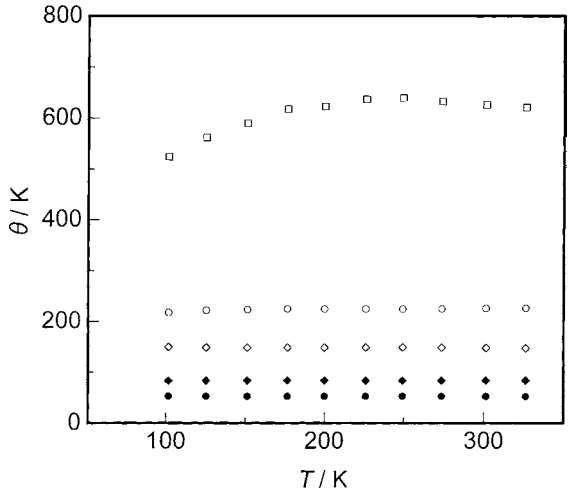

Fig. 4. The best-fit parameter values as functions of the data-set used for fitting $Pb_{1.424}Sn_{0.576}P_2Se_6$. The horizontal axis represents the upper end temperature of the interval of the data-set. The lower end temperature was 13 K for all the points. Probable errors are roughly equal to the size of the circles.

between 10 and 330 K for $Pb_{1.424}Sn_{0.576}P_2Se_6$. The Debye terms ($\Theta_{Di}(1) = 55.0 \pm 0.3$ K and 53.0 ± 0.3 K, for $Pb_2P_2Se_6$ and $Pb_{1.424}Sn_{0.576}P_2Se_6$) represent the acoustic branches of the lattice vibration and the Einstein terms optical branches, i.e. relative motions of the molecular ions. The highest frequency modes $\Theta_{Ei}(1)$ (= 500–700 K) represent the intramolecular stretching vibrations of the $P_2Se_6^{4-}$ ions. $\Theta_{Ei}(2)$, $\Theta_{Ei}(3)$ and $\Theta_{Ei}(4)$ show the torsional and translational vibrations of the molecular ions. However, precise correspondence should not be expected to hold between such qualitative descriptions of the lattice vibrations and actual characteristic temperatures.

To examine the accuracy of the model heat capacity function, we varied the temperature interval of the data taken into the least squares calculation. If the model function is an accurate representation of the actual lattice spectrum, the parameter values should be stable for different temperature intervals. This is actually the case. Figs. 3 and 4 show the best fit parameter values

Table A.1
Standard thermodynamic functions of $Pb_2P_2Se_6$ (R = 8.31451 J K^{-1} mol^{-1})

T (K)	C_p°/R	$(H^\circ - H_0^\circ)/RT$	$(S^\circ - S_0^\circ)/R$	$-(G^\circ - H_0^\circ)/RT$
10	1.074	0.2685	0.3580	0.0895
15	2.604	0.7801	1.069	0.2866
20	4.373	1.456	2.059	0.6029
25	6.142	2.217	3.225	1.009
30	7.845	3.014	4.497	1.483
35	9.456	3.820	5.829	2.008
40	10.95	4.620	7.190	2.571
45	12.32	5.401	8.561	3.160
50	13.55	6.155	9.924	3.768
60	15.64	7.569	12.59	5.018
70	17.29	8.844	15.13	6.282
80	18.63	9.986	17.53	7.539
90	19.74	11.01	19.79	8.775
100	20.69	11.93	21.92	9.984
110	21.52	12.77	23.93	11.16
120	22.26	13.53	25.83	12.30
130	22.93	14.23	27.64	13.42
140	23.53	14.87	29.36	14.49
150	24.07	15.46	31.00	15.54
160	24.57	16.02	32.57	16.56
170	25.02	16.53	34.08	17.54
180	25.44	17.02	35.52	18.50
190	25.82	17.47	36.91	19.43
200	26.17	17.90	38.24	20.34
210	26.48	18.30	39.52	21.22
220	26.78	18.68	40.76	22.08
230	27.05	19.04	41.96	22.92
240	27.30	19.38	43.11	23.74
250	27.53	19.70	44.23	24.54
260	27.74	20.00	45.32	25.32
270	27.94	20.29	46.37	26.08
273.15	28.06	20.38	46.69	26.31
280	28.13	20.57	47.39	26.82
290	28.30	20.83	48.38	27.55
298.15	28.43	21.04	49.17	28.13
300	28.46	21.08	49.34	28.26
310	28.61	21.32	50.28	28.95
320	28.76	21.55	51.19	29.63

Table A.2
Standard thermodynamic functions of $Pb_{1.424}Sn_{0.576}P_2Se_6$ (R = 8.31451 J K^{-1} mol^{-1})

T (K)	C_p°/R	$(H^\circ - H_0^\circ)/RT$	$(S^\circ - S_0^\circ)/R$	$-(G^\circ - H_0^\circ)/RT$
10	1.110	0.2776	0.3701	0.0925
15	2.559	0.7855	1.081	0.2957
20	4.284	1.442	2.050	0.6029
25	6.062	2.188	3.198	1.010
30	7.787	2.979	4.456	1.478
35	9.415	3.783	5.781	1.998
40	10.92	4.582	7.137	2.555
45	12.29	5.364	8.504	3.140
50	13.52	6.119	9.864	3.745
60	15.60	7.533	12.52	4.987
70	17.25	8.808	15.05	6.246
80	18.58	9.949	17.45	7.498
90	19.69	10.97	19.70	8.730
100	20.64	11.89	21.83	9.934
110	21.47	12.73	23.83	11.11
120	22.20	13.49	25.73	12.25
130	22.87	14.18	27.54	13.36
140	23.47	14.82	29.25	14.43
150	24.01	15.42	30.89	15.47
160	24.51	15.97	32.46	16.49
170	24.97	16.49	33.96	17.47
180	25.39	16.97	35.40	18.43
190	25.77	17.42	36.78	19.36
200	26.12	17.85	38.11	20.26
210	26.44	18.25	39.39	21.14
220	26.74	18.63	40.63	22.00
230	27.01	18.99	41.82	22.84
240	27.27	19.33	42.98	23.65
250	27.50	19.65	44.10	24.45
260	27.72	19.96	45.18	25.22
270	27.92	20.25	46.23	25.98
273.15	28.05	20.34	46.55	26.21
280	28.11	20.53	47.25	26.72
290	28.29	20.79	48.24	27.45
298.15	28.47	21.00	49.03	28.03
300	28.45	21.04	49.20	28.16
310	28.61	21.29	50.14	28.85
320	28.75	21.52	51.05	29.53
330	28.89	21.74	51.93	30.20

as functions of the upper limit temperature of the fitting interval. The Debye temperature and three lower Einstein temperatures are remarkably constant versus the change in the data-set used for the setting. This gives a strong credibility to the fitting procedure. The highest Einstein temperatures are dependent on the least squares fitting interval. These terms contribute only weakly for $T < 200\,\mathrm{K}$.

In a previous paper, we showed that the transition entropy of $10.0\,\mathrm{JK^{-1}\,mol^{-1}}$ is consistent with an order–disorder mechanism for the transitions in $Sn_2P_2Se_6$·[16] The present result for the isomorphous $Pb_2P_2Se_6$ suggests an ordered structure for this compound. This poses an interesting problem on how the ordered and disordered structures can be isomorphous with each other.

4. Conclusion

The calculation presented in this paper is an attempt to systemize and simplify the use of the Debye and Einstein functions to be tested against the experimental data. The fitting trial using simple heat capacity functions succeeded over a wide temperature range in these ionic crystals and their solid solution.

Appendix

Standard thermodynamic functions were calculated from the heat capacity data and are given in Tables A.1 and A.2 for $Pb_{1.424}Sn_{0.576}P_2Se_6$ and $Pb_2P_2Se_6$, respectively.

References

[1] A. Einstein, Ann. Phys. 22 (1908) 180.
[2] P. Debye, Ann. Phys. 39 (1912) 789.
[3] A.A. Maradudin, E.W. Montroll, G.H. Weiss, in: F. Seitz, D. Turnbull (Eds.), Theory of Lattice Dynamics in the Harmonic Approximation, Academic Press, New York, 1963.
[4] T. Matsuo, N. Kinami, H. Suga, Thermochim. Acta 267 (1995) 421.
[5] C.D. Carpenter, R. Nitsche, Mat. Res. Bull. 9 (1974) 1097.
[6] T.K. Parsamyan, S.S. Khasanov, V.Sh. Shekhtman, Yu.M. Vysochanskii, V.Yu. Slivka, Sov. Phys. Solid State 27 (1985) 2003 (Fiz. Zverd Tela 27 (1985) 3327).
[7] R. Israel, R. De Gelder, J.M.M. Smits, P.T. Beurskens, S.W.H. Eijt, T. Rasing, H. Van Kempen, M.M. Maior, S.F. Motriya, Z. Kristallogr. 213 (1998) 34.
[8] Yu.M. Vysochanskii, M.I. Gurzan, B.M. Koperles, V.Yu. Slivka, D.V. Chepur, Ukr. Fiz. Zhr. 24 (1979) 1760.
[9] J. Matas, P. Gillet, Y. Ricard, I. Martinez, Eur. J. Mineral. 12 (2000) 703.
[10] A.F. Guillermet, G. Grimvall, Phys. Rev. B 44 (1991) 4332.
[11] T. Matsuo, H. Suga, Thermochim. Acta 88 (1985) 149.
[12] T. Matsuo, Thermochim. Acta 163 (1990) 57.
[13] R.J. Borg, D.J. Dienes, The Physical Chemistry of Solids, Academic Press, New York, 1992 (Chapter 3).
[14] T. Matsuo, N. Tanaka, O. Yamamuro, A. Inaba, Netsusokutei 29 (2002) 152.
[15] T.H.K. Barron, G.K. White, Heat Capacity and Thermal Expansion at Low Temperatures, Kluwer Academic Publishers, New York, 1999.
[16] K. Moriya, H. Kuniyoshi, K. Tashita, Y. Ozaki, S. Yano, T. Matsuo, J. Phys. Soc. Jpn. 67 (1998) 3505.